

# INTERNATIONAL SOCIETY FOR SOIL MECHANICS AND GEOTECHNICAL ENGINEERING



*This paper was downloaded from the Online Library of the International Society for Soil Mechanics and Geotechnical Engineering (ISSMGE). The library is available here:*

<https://www.issmge.org/publications/online-library>

*This is an open-access database that archives thousands of papers published under the Auspices of the ISSMGE and maintained by the Innovation and Development Committee of ISSMGE.*

# Analysis and Performance of a Reinforced Soil Wing Wall Constructed over Treated Soft Ground

Bosco Poon, Kim Chan

*GHD Geotechnics, Sydney, NSW, Australia (Formerly Coffey Geotechnics)*

Richard Kelly

*Coffey Geotechnics Pty Ltd, Sydney, NSW, Australia*



2011 Pan-Am CGS  
Geotechnical Conference

## ABSTRACT

A novel remedial design solution was developed to construct a reinforced soil wing wall on soft soil treated with nonconforming short dynamic replacement columns. The solution comprised (i) a detached connection system to allow for greater tolerable movement of the wing wall, (ii) installation of stone columns underneath the reinforced soil block as well as the wall facing, and (iii) the use of a dead-man anchorage system to tie-back the ground beam that underpins the wall facing. This paper focuses on the numerical analysis of the remedial wing wall system, and compares its prediction with actual performance.

## RÉSUMÉ

Dans le cadre d'un projet d'installation d'un mur en terre armée sur du sol mou, il a été proposé d'utiliser un système de fondation reposant sur l'utilisation d'un réseau d'inclusions rigides installés par la méthode de plots de colonnes ballastés. La solution consiste en (i) une connection flexible permettant une plus grande mobilité du mur incliné, (ii) l'installation de colonnes ballastées en dessous du bloc de terre armée de même que les parements du mur, et (iii) l'utilisation d'un système de tirants passifs pour retenir la semelle filante du mur de parement. Cet article se penche sur l'analyse numérique du système de mur incliné, et compare le comportement théorique du mur avec le comportement observé.

## 1 INTRODUCTION

As part of the ongoing program of works to upgrade the Pacific Highway that connects Sydney to Brisbane, the Ballina Bypass Alliance was established in September 2007 to construct a 11.5km-long four-lane dual carriageway to divert the traffic away from the township of Ballina. The northern end of the Ballina Bypass, known as Upper Sandy Flat, lies in a valley where soft estuarine soils have been deposited. The soft soil thickness is up to 5m, and the maximum design embankment height is about 9m. The ground treatment measures adopted at the design stage for this area comprised dynamic replacement (DR) columns with wick drains and surcharge.

A 16m span arch culvert is proposed to underlie an 8m high embankment. The culvert is flanked by two reinforced soil wing walls at the northern (Wing Wall A) and southern end (Wing Wall C) as shown in Figure 1. The arch culvert structure is supported by a piled foundation whereas the wing walls were originally designed to be a reinforced soil wall (RSW) founding on full depth DR columns that are installed to the base of the soft soil. The wall facing was positioned to be located between two rows of DR columns and a standard levelling pad was used to support the wall facing panels. Prior to the construction of the arch culvert and the RSW wing walls, a post-DR investigation indicated that many of the DR columns at the wing wall locations were not installed to their design depth, and the untreated soft soil thickness beneath the short DR columns was in excess of 0.5m. This may result in total and differential wall movements exceeding the design criteria. A novel remedial solution with value for money consideration was subsequently

developed to remediate the RSW wing walls without opting for hard treatment options such as piled foundation. This solution comprised (i) a detached connection system to allow for greater tolerable movements between the wing wall and the spandrel wall of the arch structure; (ii) installation of stone columns (SC) underneath the reinforced soil block as well as the wall facing to reduce settlement and lateral spreading; and (iii) the use of dead-man anchor to prevent excessive yielding of the front row of DR columns supporting the wall facing.

This paper focuses on the numerical analysis of the remedial wing wall system, and compares its prediction with actual performance under short term loading conditions.

## 2 GROUND CONDITIONS

The geotechnical model adopted for the wing wall areas included subsurface stratigraphy and geotechnical parameters. The subsurface stratigraphy was derived from field investigations comprising electric friction cone tests (CPT), piezocone tests (CPTU) and boreholes. Geotechnical parameters were assessed from interpretation of the field and laboratory test results. It was assessed that the subsoil conditions at Wing Walls A and C exhibit similar characteristics and can be represented by a single geotechnical model shown in Table 1. The corresponding profiles of inferred undrained shear strength ( $s_u$ ) and over-consolidation ratio (OCR) are shown in Figure 2. The salient features of the soil model are summarised as follows:

- The soft soil deposit comprises high plasticity clay with a liquid limit  $w_L$  of between 78% and 88%. The plasticity index  $I_P$  is about 50%.

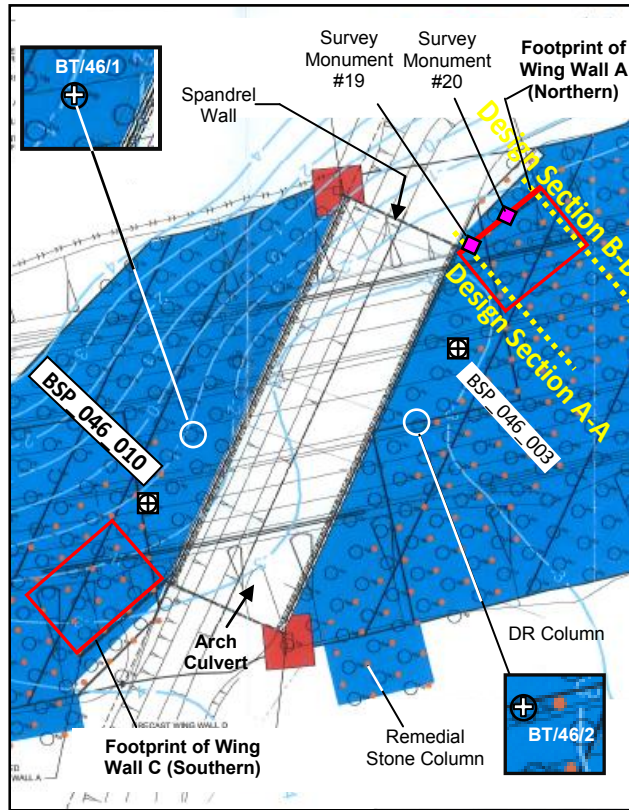


Figure 1. Ground treatment and monitoring plan

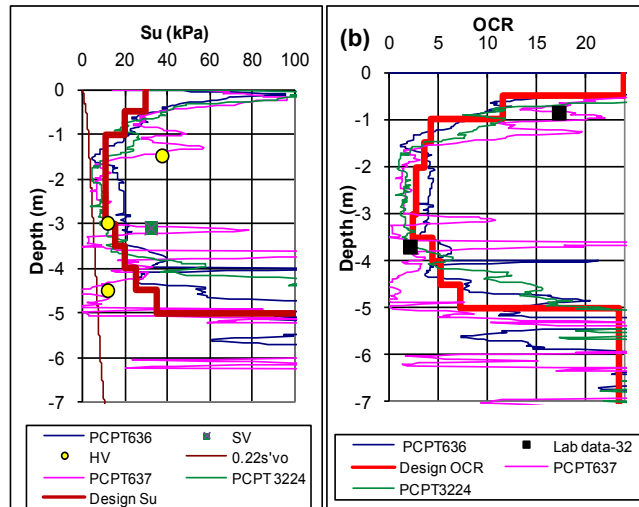


Figure 2. Undrained Shear Strength and OCR Profiles

- The derivation of the  $s_u$  profile with depth was estimated from the measured piezocone data using  $N_{kt}$  value of about 15. The adopted  $N_{kt}$  value has been calibrated against corrected vane shear data.
- The adopted design OCR profile is consistent with the adopted design  $s_u$  profile through the relationship proposed by Ladd (1991):

$$s_u = S(OCR)^m \sigma'_{vo} \quad s_u = S(OCR)^m \sigma'_{vo} \quad (1)$$

where  $S = 0.20 + 0.05 I_p$  ( $\sim 0.22$  for  $I_p = 0.5$ );  $m = 0.88(1 - CRR/CR) \pm 0.06$  ( $\sim 0.8$  for  $CR/CRR = 7$ ); and  $\sigma'_{vo}$  is the vertical effective stress. In addition, the design OCR profiles compare reasonably well with the OCR values obtained from oedometer tests via the conventional Casagrande (1936) technique (See Figure 2b).

- The coefficients of consolidation  $c_h$  (horizontal) were derived based on pore pressure dissipation test within the CPTU. The adopted  $c_v$  (vertical) was taken to be half of the  $c_h$  values. Note that  $c_v$  and  $c_h$  derived from piezocone are significantly higher than those from the oedometer test results. The laboratory results were however considered to be too conservative since the testing sample may have been subject to disturbance.

Table 1. Geotechnical Model and Design Parameters

| Layer | Thick-ness | CR <sup>(1)</sup> | CRR <sup>(2)</sup> | OCR  | $c_h$              | $\gamma$          | $s_u$ |
|-------|------------|-------------------|--------------------|------|--------------------|-------------------|-------|
| —     | m          | —                 | —                  | —    | m <sup>2</sup> /yr | kN/m <sup>3</sup> | kPa   |
| 1     | 0.5        | 0.2               | 0.03               | 70   | 20                 | 18                | 30    |
| 2     | 0.5        | 0.35              | 0.05               | 11.6 | 5                  | 15                | 20    |
| 3     | 0.5        | 0.35              | 0.05               | 4.3  | 5                  | 14.5              | 11    |
| 4     | 0.5        | 0.35              | 0.05               | 3.6  | 5                  | 14.5              | 11    |
| 5     | 1          | 0.35              | 0.05               | 2.8  | 5                  | 14.5              | 11    |
| 6     | 0.5        | 0.35              | 0.05               | 2.4  | 5                  | 14.5              | 15    |
| 7     | 0.5        | 0.35              | 0.05               | 4.5  | 5                  | 14.5              | 20    |
| 8     | 0.5        | 0.3               | 0.05               | 5.3  | 5                  | 15                | 25    |
| 9     | 0.5        | 0.3               | 0.05               | 7.3  | 5                  | 15                | 35    |
| 10    | 4.5        | 0.1               | 0.015              | 23.5 | 50                 | 19                | 150   |

Note to Table 1:

- (1) CR = compression ratio =  $C_c/(1+e_o)$
- (2) CRR = recompression ratio =  $C_r/(1+e_o)$
- (3)  $\gamma$  = bulk unit weight

### 3 GROUND TREATMENTS

Following preliminary assessment of a number of ground improvement options including deep soil mixing and rigid inclusion methods, it was decided to adopt dynamic replacement (DR) as the preferred ground improvement solution due to its relative speed of construction and economy. To meet the stringent post-construction settlement criteria for the general embankment area at Upper Sandy Flat, it was also necessary to surcharge the site. Prefabricated wick drains were installed after the formation of DR to increase the rate of consolidation even though the DR columns would already facilitate radial drainage in the soft clay.

Dynamic Replacement columns are introduced into the ground by a heavy weight dropped repeatedly onto a gravel layer while the craters created by the impact of the heavy weight are backfilled with gravel. The resulting DR columns are relatively large in diameter, have high load carrying capacity, and are rapid to install. The disadvantage of DR, however, is that there is a limiting depth to which the DR columns can be installed. The maximum depth of penetration of the DR columns through the top of the 1.2m thick working platform at Upper Sandy Flat was assessed to be about 5.5m, thereby leaving about 0.7m thickness of the soft clay (for a total soft clay thickness of 5m) untreated. It was also assessed that many of the DR columns at the wing wall areas did not fully penetrate to the soft soil base. Additional ground

treatment using stone columns was subsequently introduced to remediate the untreated soft soil below DR columns. The final treatment solutions are summarised in Table 2 and shown in Figures 1 and 3. Instrumentation was installed and monitoring carried out to confirm the design assumptions and to enable decisions to be made on when the surcharge could be removed. Instrumentations that are relevant to the wing walls are shown in Figure 1. These include two settlement plates (BSP\_046\_003 and BSP\_046\_010) located behind Wing Walls A and C; and two pressure cells (BT/46/1 and BT46/2) installed at the top of two floating DR columns near the arch culvert to measure the imparted vertical stress. The horizontal and vertical movements of the wing walls were measured by survey monuments placed on the ground beam of the wing walls (see Section 4).

Table 2. Adopted Ground Treatments at Upper Sandy Flat

| Ground Treatment  | Details   |
|-------------------|---|
| DR column         | Nominally 2.5m in diameter; 5m equilateral triangular spacing; Area replacement ratio <sup>(1)</sup> , $a_r = 23\%$ |
| Stone Column (SC) | Nominally 1m diameter; 5m equilateral triangular spacing; Area replacement ratio <sup>(1)</sup> , $a_r = 3.6\%$     |
| Wick Drain        | Installed after DR formation at 1.2m equilateral triangular spacing   |

Note to Table 2:

- (1) The area replacement ratio is defined as the ratio of the cross-sectional area of one column to the total cross-sectional area of the 'unit cell' attributed to each column

#### 4 REINFORCED SOIL WALL DESIGN

While the total fill behind the RSW is at constant height of 10.5m, the design wall height varies linearly from a lowest end of about 3.6m to a top end of about 7m next to the spandrel wall of the arch culvert unit. There is no shear connection between the wing wall and the spandrel wall to allow movements of the wing wall. The gap at the detached connection is sealed with deformable material in conjunction with geotextile. The following design criteria were incorporated in the wing wall design: (i) maximum allowable differential movements (both vertically and horizontally) for the wall face of 1.0 percent change in grade to prevent cracking of wall panels; and (ii) Maximum horizontal movement of the wall face of 150mm over 100 years to avoid potential closure of the 170mm clearance at the wing wall / spandrel wall juncture.

The design configuration of the reinforced soil wing wall for the required criteria is outlined in Figure 3. In essence, the reinforced soil block is 12m wide and is built upon a stripped 0.75m thick working platform that was constructed over the DR and remedial SC columns. To limit the total and differential settlements of the wall facing, a ground beam spanning over a row of remedial stone columns is provided to support the precast wall panels. To limit the applied horizontal force on the supporting stone columns which are geotechnical elements without significant bending stiffness, a dead-man anchorage system is adopted to tie back the ground

beam into the platform fill. The dead-man anchor block is a continuous beam with dimension 1.25m (H) × 1m (W). The anchor bars that connect the ground beam and the dead-man block are 20m long 32mm diameter stress-bar at a horizontal spacing of 3m.

Survey monuments were introduced at the ground beam to monitor wall-face movements. Typical monument location plan for Wing Wall A is shown in Figure 1.

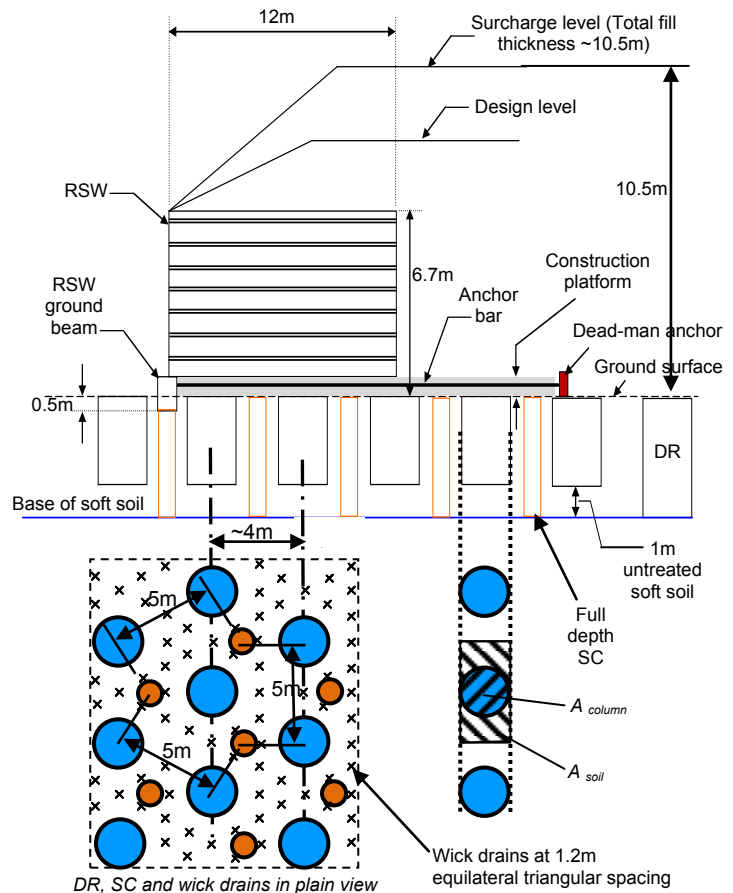


Figure 3. Reinforced soil wing wall design configuration

The dead-man anchor also assists the overall stability against sliding of the reinforced soil block. If the reinforced soil wall was built without the dead-man anchor, the reinforced soil block would need to be embedded for the required sliding resistance. The soil excavation within the reinforced soil block footprint may be subject to construction and/or environmental constraints including (i) water inflow during excavation, (ii) damage of the DR and SC columns and (iii) disposal of excavated soft soil. For the proposed wing wall design, the RSW and the anchored ground beam can be considered as a single soil reinforcement unit and a minimum embedment of this unit can be achieved by embedding the ground beam to 0.5m below ground surface without excavating the entire reinforced soil block area.



## 5 PERFORMANCE PREDICTION APPROACH

The modelling of the reinforced soil wing wall was carried out based on two-dimensional (2D) finite element analyses (FEA). However, due to the three-dimensional (3D) nature of the installed SC/DR columns, a separate 3D FEA was undertaken for a sample group of SC/DR columns to assess the equivalent 2D column stress concentration parameters. The 3D group analysis also involved coupled consolidation to assess the time for the stabilisation of the wall movements, which could be difficult to be carried out in a 2D FEA. The details of the design methodology are discussed below.

In the modelling of the wing wall, the total and differential wall movements were assessed by carrying out 2D FEA using PLAXIS software programme at two cross-sections along Wing Wall A as shown in Figure 1, for the wall heights and retaining fill heights summarised in Table 5. The design analyses have only been carried out for Wing Wall A, but the results are deemed to be directly applicable for Wing Wall C due to their similar wall heights and sub-soil profiles.

Conventionally, the design of SC/DR columns involves the prediction of their settlements using a composite material approach in which equivalent strength and deformation parameters are derived using semi-empirical correlation to represent the entire treated soil. For the current problem, however, the key design criteria are horizontal displacements. The above composite material approach, while has been accepted as a reasonable method for vertical displacement prediction, is less certain for the prediction of horizontal displacement. The adopted design approach was to explicitly model the SC/DR as strips in the 2D FE model with the appropriate diameter, spacing and smeared properties of the columns.

In the 2D FE model, the soft clays were modelled using Soft Soil Model in the PLAXIS programme, which resembles the Modified Cam-Clay model with a Mohr-Coulomb hexagon yield surface in the deviatoric plane. The adopted model parameters have been given in Table 1. For the purpose of analysis, it was assumed that 6 rows of short DR columns reside below the wing wall with up to 1m thick untreated soft soil beneath the columns; 5 rows of remedial full depth SC were also modelled in between the short DR columns. The widths of the DR and SC strips were the same as their actual diameter (i.e. 2.5m and 1m respectively), but the strip spacing was 4m instead of the actual 5m spacing because of the triangular configuration as shown in Figure 3. The DR/SC strips were modelled as Mohr-Coulomb materials with adopted Poisson ratio of 0.3, which was taken to be the value for the soil itself. The equivalent Young's modulus,  $E_{eq}$ , of the DR/SC strips can be calculated based on weighted average approach as given by Equation 2:

$$E_{eq} = \frac{E_{soil}A_{soil} + E_{col}A_{col}}{A_{soil} + A_{col}} \quad (2)$$

$$E_{eq} = \frac{E_{soil}A_{soil} + E_{col}A_{col}}{A_{soil} + A_{col}}$$

where  $A_{soil}$  and  $A_{col}$  are the areas of the soil and the column inside a unit cell within the DR/SC strips as shown in Figure 3. The design Young's moduli of SC/DR

columns ( $E_{col}$ ) are given in Table 4 and the adopted soil Young's modulus ( $E_{soil}$ ) was 1.7MPa, which was approximately equal to 150 times the undrained shear strength,  $S_u$ , of 11kPa.

The equivalent friction angle,  $\phi_{eq}$ , of the DR/SC strips can be derived based on force equilibrium approach as given by Equation 3:

$$\tan(\phi_{eq}) = \frac{A_{soil} \tan(\phi_{soil}) + n \cdot A_{col} \tan(\phi_{col})}{A_{soil} + n \cdot A_{col}} \quad (3)$$

where the adopted friction angle of the columns are given in Table 4; the adopted soil friction angle was 25°; and  $n$  was the stress concentration factors over the SC and DR columns (i.e. column stress / soil stress). The stress concentration factor is one of the most difficult parameters to establish and may not be able to estimate adequately using published correlations due to (i) combination of full depth SC and short DR columns at the site; (ii) uncertainty in the degree of yielding in the SC/DR columns; and (iii) in-homogeneity of soft soil layers. In the design analysis, the stress concentration factors were assessed separately by carrying out a full 3D FEA (using PLAXIS 3D Foundation software programme) for a group of SC/DR columns under axially symmetric condition as shown in Figure 4.

The salient features of the 2D FEA model, as well as the adopted construction sequences are summarised in Table 3. Note that the 2D FEA is an elasto-plastic analysis for the assessment of long term deformation in which the decay of excess pore pressure with time during the primary consolidation stage was not taken into account. It may not be easy to incorporate consolidation in the 2D plane strain analysis since it is difficult to convert the 3D vertical drain system with a combination of full depth SC, short DR and wick drains into equivalent parallel drain walls. In the design analysis, the time for consolidation was also assessed separately by carrying out a coupled consolidation analysis in the 3D modeling for the SC/DR group under 10.5m embankment fill as depicted in Figure 4. Thus the radial drainage towards the SC/DR columns, which were treated as large diameter drains with high permeability, can be modelled directly. The time for the stabilisation of the wall movements can be inferred from the time-settlement curve obtained in the 3D FEA.

One of the challenges in the consolidation analysis is the selection of soil permeability values  $k_v$  (vertical) and  $k_h$  (horizontal), which can be calculated from  $c_v$ ,  $c_h$  and the coefficient of volume change  $m_v$  (estimated from the total settlement under full embankment fill load). Owing to the installation method for the SC and DR columns, the soil surrounding the columns may have been remoulded/smeared; the  $c_v$  and  $c_h$  of the remoulded soil would be much lower than that of the in-situ state. However, it is noticed from the comparison with the monitoring data that the reduced  $c_v$  and  $c_h$  of the remoulded soil may have been compensated by the wick drains such that a reasonable agreement between measurement and prediction was obtained by adopting the in-situ  $c_v$  and  $c_h$  of a normally consolidated clay without smearing (as given in Table 1), but without the modelling the wick drains themselves (see Section 6).

Table 3. Construction sequence for 2D FEA

| Stage | Construction Operation   | Comment   |
|-------|--|---|
| 1     | Calculate initial stress for in-situ ground  | Initial in situ effective stresses were estimated from the assumed stress history (Table 1) and the expression $K_0 = (1 - \sin \phi) \sqrt{OCR}$   |
| 2     | Install construction platform and SC/DR columns  | The SC/DR strips were 'wished in place'; No installation effects have been considered. The smeared SC/DR properties are assessed from Equations 2 and 3, in conjunction with the stress concentration factors obtained from a separate 3D FEA.  |
| 3     | Construct ground beam and dead-man anchor  | The Ground beam and dead-man anchor were represented by linear elastic material with $E' = 32\text{GPa}$ and $\nu = 0.15$ . The anchor bars were modelled using two-node elastic spring element without pre-stressing. The long term axial stiffness of the bar was derived based on $E' = 200\text{GPa}$ and a reduced cross section sacrificial thickness of 0.85mm. The adopted stiffness value in the 2D model has been averaged over the anchor spacing in the out-of-plane direction.   |
| 4     | Reset Displacement to zero   |   |
| 5     | Construct RSW and embank. fill to top of surcharge level   | Membrane elements with limiting tensile strength were used to model reinforced strips. No slippage was allowed at the membrane face since it had been designed (based on limit equilibrium) to have its pull-out resistance > the tensile capacity. As layers of soil and reinforcement were placed at the RSW, a wall facing represented by discrete beam elements were also included. Interface elements were introduced at the soil-wall contact to allow for slippage. The roughness of the interface was assumed to be 70% of the original soil strength values. |
| 6     | Strip surcharge to design level; applied traffic surcharge for long term performance assessment. |   |

## 6 RESULTS OF ANALYSIS

### 6.1 Results of 3D group analysis for SC/DR columns

Prior to the modelling of the RSW in 2D, a pilot 3D group analysis for the SC/DR columns was carried out to assess the stress distribution between columns and soil. In addition, the 3D analysis also involved coupled consolidation such that the time for the stabilisation of wall movement can be assessed.

Figure 4 shows a slightly exaggerated deformed 3D mesh of the SC/DR columns under full embankment load. It can be seen that the full depth SC have exhibited bulging in the soft soil layer, while the floating short DR columns have undergone punching type deformation mode at the column base. The increase in vertical effective stress for the SC, DR and the surrounding soil under fill loading are shown in Figure 5. For the DR with  $a_r = 23\%$ , the effective vertical stress peaked at about 1m below existing ground level. Below this level, the imparted DR stress reduces as load is transferred from the floating DR to the surrounding soil. The adjacent SC ( $a_r = 3.6\%$ ) exhibit increased vertical effective stress with depth. It is noted that the predicted column stress of about 400kPa at the top of the short DR agrees reasonably well with the pressure cell measurements as shown in Figure 6.

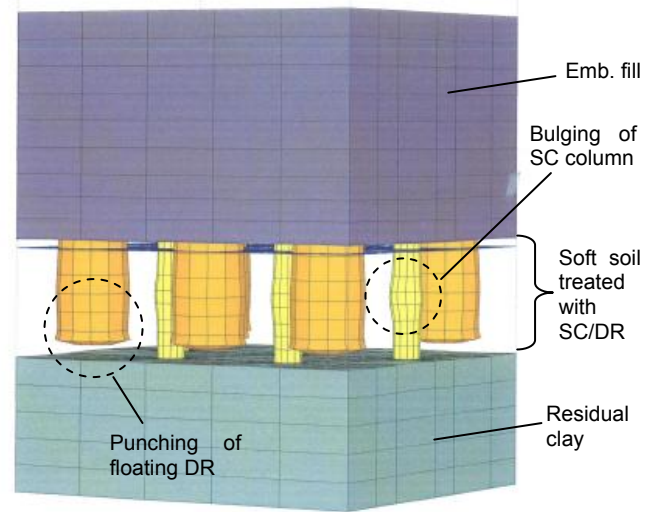


Figure 4. 3D FEA Result for a Group of SC/DR Columns

Figure 7 shows a plot of the predicted stress concentration factors  $n_{DR}$  (for DR column) and  $n_{SC}$  (for SC) versus depth. It can be seen that except for the first 1m depth,  $n_{SC}$  value is about 4.5 and it is fairly constant with depth. Due to the load transfer from the DR to the surrounding soil and SC, the  $n_{DR}$  is however reduced from a peak value of about 4.3 at 1m below ground to about 3 at the column base. In the design analysis,  $n_{SC} = 4.5$  and  $n_{DR} = 3.5$  is adopted for the derivation of equivalent friction angle,  $\phi_{eq}$ , for the SC/DR strips in the 2D modeling. The calculated  $\phi_{eq}$  are given in Table 4.

Table 4. Design parameters for SC and DR columns

| DR/SC | $n^{(1)}$ | Adopted $E'$ for column | Smeared $E'$ for strip in 2D FEA | Adopted $\phi'$ for column | Smeared $\phi'$ for strip in 2D FEA |
|-------|-----------|-------------------------|----------------------------------|----------------------------|-------------------------------------|
|       | —         | MPa                     | MPa                              | degrees                    | degrees                             |
| DR    | 3.5       | 30                      | 12.8                             | 35                         | 32                                  |
| SC    | 4.5       | 50                      | 9.3                              | 40                         | 32                                  |

Note to Table 4:

(1)  $n$  = stress concentration factor = column stress / soil stress at the same level

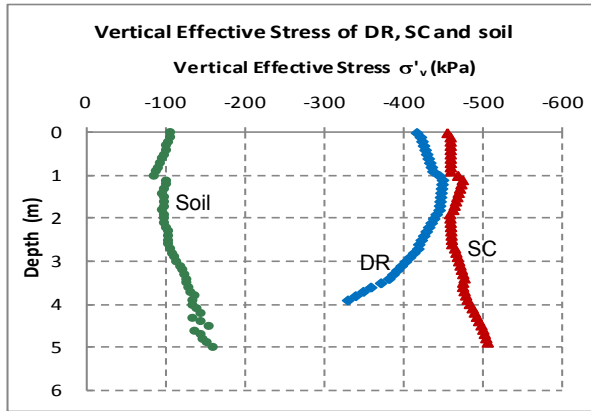


Figure 5. Vertical effective stress of DR, SC and soil

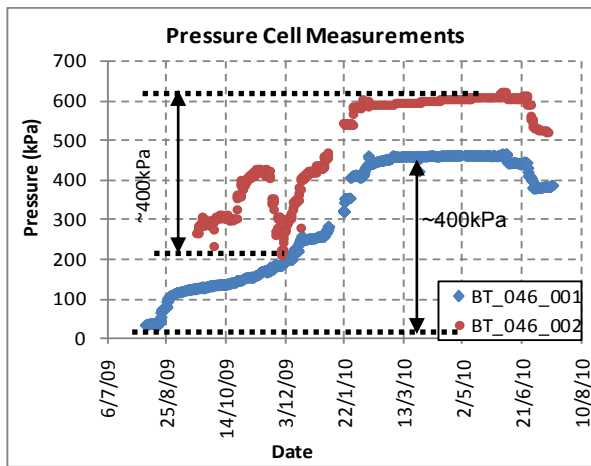


Figure 6. Pressure cell measurements (Top of short DR)

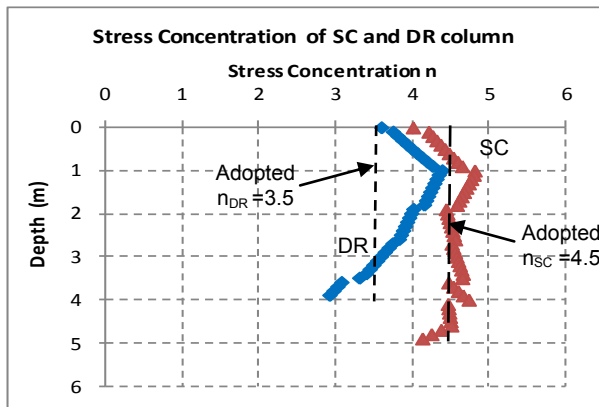


Figure 7. Stress concentration of SC and DR columns

Figure 8 shows a comparison of the predicted time-settlement response from 3D analysis and the measured data from settlement plate BSP\_046\_003. It is emphasised that the prediction is by no means obtained from back analysis, thus the agreement between the two results, especially towards the end of the consolidation, is considered quite satisfactory. A noteworthy point about the analysis is that wick drains were not included in the 3D model. However the results as shown in Figure 8

might have suggested that such an omission in the SC/DR treated ground was compensated for also not modelling smearing of the remoulded soft soil surrounding the SC/DR columns.

Due to the fact that the construction platform was built much earlier than the embankment fill, some settlement has already occurred prior to the fill placement. In the design analysis, however, the platform fill and the embankment fill were constructed at the same rate, potentially contributing to the discrepancy between the prediction and measurement at the onset of the fill loading. The assessed time for the wing wall to settle, as inferred from the time to achieve 90 percent degree of consolidation in Figure 8, is about 5.5 months from the start of fill placement.

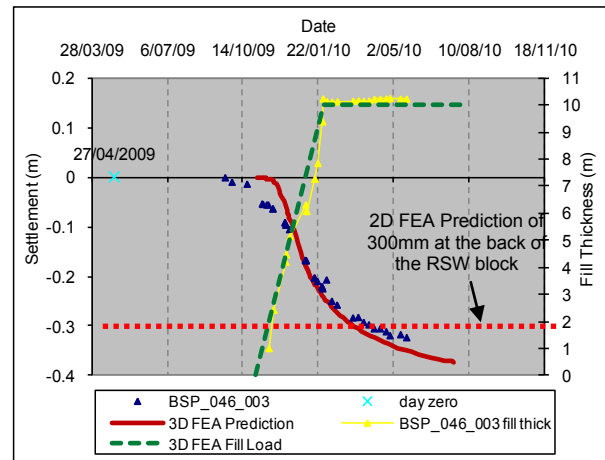


Figure 8. Time-settlement prediction from 3D FEA

## 6.2 Results of 2D analysis for Reinforced Soil Wing Wall

Before considering the numerical results of the wing wall movements, it is illuminating to discuss the deformation mechanism of the RSW and the function of the dead-man anchor. Finite element analyses have shown that lateral soil movements of the SC and adjacent soil beneath the wall facing have a direct influence on the overall performance of the wing wall design. For example, if the first row of SC supporting the wing wall ground beam is omitted, both horizontal and differential vertical movements may exceed the design criteria. However, even with the SC in place is not a complete solution since the SC, which is stiffer than the surrounding soft clay, have attracted concentrated shear stress within the column. This has resulted in lateral yielding of the column, thus undermining its effectiveness in reducing the lateral spreading under embankment load. The dead-man anchor is therefore considered to be an essential component in the wing wall design for its role to limit the applied shear force on the SC, thus greatly reducing the outward movement of the wall facing.

Figure 9 shows an exaggerated deformed mesh of the RSW Wing Wall A under short term fill load with surcharge at cross-section A-A in Figure 1. The RSW block deforms in a backward tilting mode, with the predicted settlements at the wall facing and behind the

RSW block being equal to 210mm and 300mm, respectively. These results are in good agreement with the field measurements; refer Figure 10 for settlement at wall facing and Figure 8 for settlement behind RSW block. Also note that the time for the stabilisation of the wing wall facing is about 5.5 month according to the ground beam measurement (i.e. based on Survey Monument #19, see Figure 10). This is consistent with the measured data at settlement plate BSP\_046\_003 behind the RSW block, as well as with the 3D analysis result (Figure 8). Figure 11 shows a comparison of the predicted ground beam horizontal movement from the 2D analysis and measurement. It can be seen that the prediction is about 2.2 times greater than the measured value. Several reasons may be postulated for the difference between the measured and predicted horizontal movements:

- Installation effect on undrained soil strength – The SC/DR columns in the 2D and 3D analyses were ‘wished in place’, meaning that the installation effects have been ignored. In reality, the creation of large diameter SC and DR columns may cause significant increase in the lateral effective stress of the treated soft ground, leading to a higher undrained shear strength ( $S_u$ ) value. Wong and Lacazedieu (2009) have reported that the increase in  $S_u$  due to DR installation could be up to 40kPa to 55kPa for a very soft clay at an Egypt site.
- Installation effect on anisotropic column stiffness – For the SC/SR columns that are formed by granular materials, the increase in horizontal to vertical effective stress ratio ( $\sigma'_h/\sigma'_v$ ) due to column installation may increase the degree of anisotropy of the column stiffness ( $E_h/E_v$ ). This anisotropic behaviour has been shown by Kohata et al. (1997) for a range of sands and gravels.
- The use of reduced anchor bar stiffness – As indicated in Table 3, the anchor bar was modelled using a long term axial stiffness ( $EA/L$ ) that account for a sacrificial thickness of 0.85mm. This may however underestimate the axial stiffness for the short term.
- It is well established in literature (e.g. Poulos 1972) that it is difficult to achieve reliable predictions of lateral movements under an embankment, especially after the end of construction.

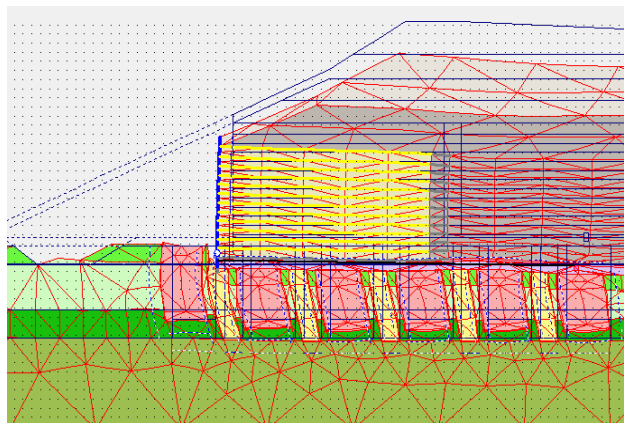


Figure 9. 2D FEA result for Wing wall A, cross-section A-A

Table 5 summarises the performance predictions under short term surcharge loading, as well as presenting some of the measured data from monitoring results. Table 6 summarises the predictions for the maximum reaction forces of the ground beam and anchor bar, which are within their structural capacities. A free body diagram showing the reaction forces is given in Figure 12. It is noted that while design cross-section A-A can be compared with measurements from survey monument #19 because of their similar locations, the design cross-section B-B is about 7.5m south of survey monument #20 and therefore they cannot be compared directly due to the different wall heights at the two locations. In terms of differential wall movements, the predicted results are in good agreement with the measurements both vertically and horizontally. Overall, it can be seen that the design predictions are reasonable with regard to settlement and differential movements (both vertical and horizontal). The prediction for the total horizontal movement is however erring on the conservative side, although it remains within the design limit of 150mm.

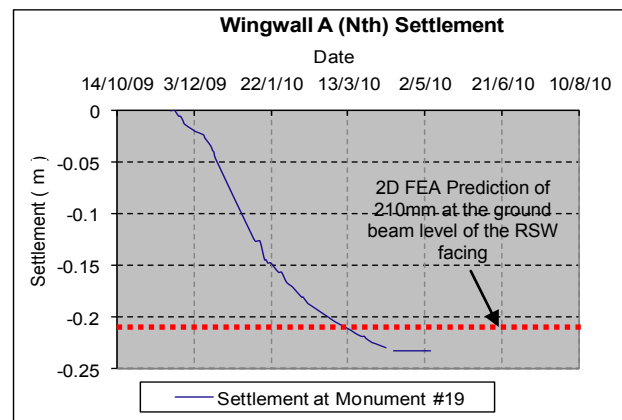


Figure 10. Measured and predicted settlement at Wing Wall A facing

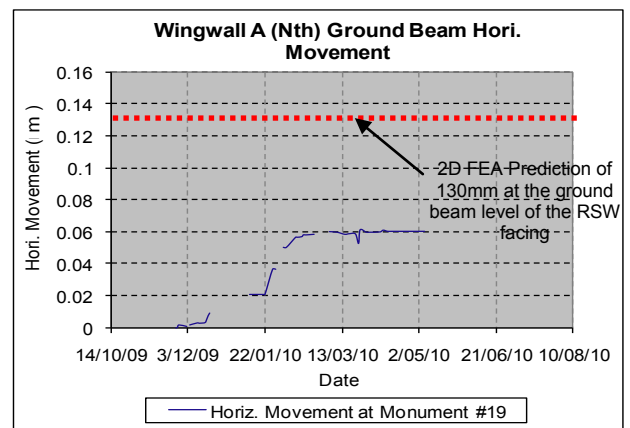


Figure 11. Measured and predicted horizontal movement at ground beam level of Wing Wall A facing



Table 5. Summary of Wing Wall A movements under short term construction loading

| Cross section /Monument             | Prediction   |      | Measurement  |      |
|-------------------------------------|--|------|--|------|
|                                     | A-A  | B-B  | #19  | #20  |
| Wall height (m)                     | 6.7  | 4.0  | 6.7  | 5.2  |
| Total Fill height behind batter (m) | 10.5   | 10.5 | 10.5   | 10.5 |
| Settlement (mm)                     | 210  | 160  | 230  | 210  |
| Hori. movement at wall base (mm)    | 130  | 100  | 60   | 45   |
| Differential settlement             | 50mm settlement over 15m between Sections A-A and B-B; or 0.33% change in grade      |      | 20mm settlement over 7.5m between Monuments #19 and #20; or 0.27% change in grade      |      |
| Differential horizontal movement    | 30mm lateral movement over 15m between Sections A-A and B-B; or 0.2% change in grade |      | 20mm lateral movement over 7.5m between Monuments #19 and #20; or 0.2% change in grade |      |

Table 6. Maximum reaction forces of ground beam and anchor bar

| Reaction force                                | Force per unit length          |
|---|--------------------------------|
| Vertical force on ground beam top ( $B_v$ )   | 60kN/m                         |
| Horizontal force on ground beam top ( $B_H$ ) | 73kN/m                         |
| Tensile force of anchor bar (spaced at 3m)    | 323kN per bar or 108kN/m (SLS) |

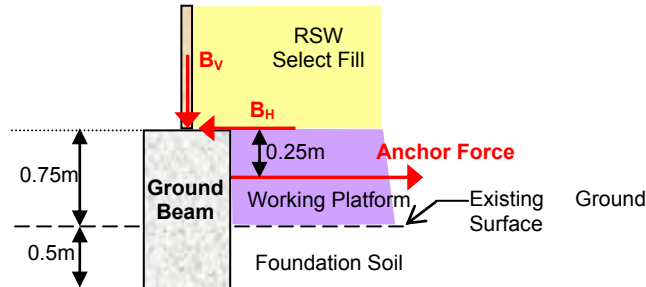


Figure 12. Reactions of ground beam and anchor bar

## 7 CONCLUSIONS

Owing to the DR columns not installed to their design depths at Upper Sandy Flat, a remedial design has been carried out for the two reinforced soil wing walls at this location. The remedial work commenced by firstly identifying the most appropriate settlement criteria for the wing wall design. This was achieved by close collaboration between structural and geotechnical engineers in pursuit of the detached connection system that allows for maximum tolerable movements between the wing wall and the spandrel wall of the arch culvert. This has made possible a more economical remedial solution using stone columns in conjunction with dead-man anchor without wandering into the hard treatment options such as piled foundation.

A 2D FEA has been carried out to model the reinforced soil wing wall. One of the key features in the 2D analysis is the modelling of the SC/DR columns as equivalent strips. The 2D analysis was also supplemented by a separate 3D coupled FEA that was used to simulate the behaviour of a group of SC/DR columns under axially symmetric loading condition. The objective of the 3D analysis was to assess (i) the stress distribution of the SC/DR columns, which is essential for calculating the equivalent strength parameters for the SC/DR strips in the 2D analysis; and (ii) the time for the stabilisation of wall movement.

The analysis predictions have been compared with field measurements and the following observations and conclusions can be drawn:

- The stress distribution between SC/DR columns and soil has been obtained from the 3D group analysis. The predicted column stresses have shown reasonably good agreement with the pressure cell measurements at the top of the DR columns.
- Although wick drains and smearing effect were not included in the 3D coupled analysis, the predicted time-settlement response has compared favourably with the settlement plate measurements. This may suggest that the wick drains serve to compensate for the slow down due to smearing of the remoulded soil surrounding the SC/DR columns.
- In general the 2D FEA has given satisfactory wall movement predictions with regard to settlement and differential wall movements (both vertical and horizontal). The prediction for the total horizontal movements is however erring on the conservative side, and it remains within the design limit of 150mm.

## ACKNOWLEDGEMENTS

The writers would like to acknowledge the Roads and Traffic Authority (RTA) of New South Wales at the Ballina Bypass Alliance for their kind permission to use the data for the preparation of this paper.

## REFERENCES

- Casagrande, A. (1936). "The determination of the pre-consolidation load and its practical significance." Proc. 1<sup>st</sup> ICSMFE, Cambridge, 3, 60-64.
- Kohata Y., Tatsuoka F., Wang L., Jiang G.L., Hoque E. & Kodaka T (1997), "Modelling of nonlinear deformation properties of stiff geomaterials." Geotechnique, Vol. 47, No. 3, pp 563-580.
- Ladd, C.C. (1991). "Stability evaluation during staged construction: 22<sup>nd</sup> Terzaghi Lecture." Jnl of Geot Eng, ASCE, 117(4), 537-615.
- Poulos, H.G. (1972). "Difficulties in prediction of horizontal deformations of foundations." J. Soil Mech. Found. Div., Proc. ASCE, 98 (SM8), 843-848.
- Wong, P.K. and Lacazedieu, M. 2004. "Dynamic replacement ground improvement – Field performance versus design predictions for the Alexandria City Centre Project in Egypt." Advances in Geotechnical Engineering. The Skempton Conference. Vol 2 pp 1193 - 1204